Chin. Geogra. Sci. 2019 Vol. 29 No. 6 pp. 949–961
https://doi.org/10.1007/s11769-019-1079-2

Springer Science Press
www.springerlink.com/content/1002-0063

Siting of Dark Sky Reserves in China Based on Multi-source Spatial Data and Multiple Criteria Evaluation Method

WEI Ye[1], CHEN Zuoqi[2, 3], XIU Chunliang[4], YU Bailang[2, 3], LIU Hongxing[5]

(1. *Key Laboratory of Geographical Processes and Ecological Security in Changbai Mountains*, *Ministry of Education*, *School of Geographical Sciences*, *Northeast Normal University*, *Changchun* 130024, *China*; 2. *Key Laboratory of Geographic Information Science* (*Ministry of Education*), *East China Normal University*, *Shanghai* 200241, *China*; 3. *School of Geographic Sciences*, *East China Normal University*, *Shanghai* 200241, *China*; 4. *College of Jang Ho Architecture*, *Northeastern University*, *Shenyang* 110169, *China*; 5. *Department of Geography*, *University of Alabama*, *Tuscaloosa*, *AL* 35487, *USA*)

Abstract: With the rapid development of population and urbanization and the progress of lighting technology, the influence of artificial light sources has increased. In this context, the problem of light pollution has attracted wide attention. Previous studies have revealed that light pollution can affect biological living environments, human physical and mental health, astronomical observations and many other aspects. Therefore, organizations internationally have begun to advocate for measures to prevent light pollution, many of which are recognized by the International Dark-Sky Association (IDA). In addition to improving public awareness, legal protections, technical treatments and other means, the construction of Dark Sky Reserves (DSR) has proven to be an effective preventive measure. So far, as a pioneer practice in this field, the IDA has identified 11 DSRs worldwide. Based on the DA requirements for DSRs, this paper utilizes NPP-VIIRS nighttime light data and other multi-source spatial data to analyze possible DSR sites in China. The land of China was divided into more than ten thousand 30 km × 30 km fishnets, and constraint and suitable conditions were designated, respectively, as light and cloud conditions, and scale, traffic and attractiveness conditions. Using a multiple criteria evaluation, 1443 fishnets were finally selected as most suitable sites for the construction of DSRs. Results found that less than 25% of China is not subject to light pollution, and less than 13% is suitable for DSR construction, primarily in western and northern areas, including Tibet, Xinjiang, Qinghai, Gansu and Inner Mongolia.

Keywords: Dark Sky Reserves; light pollution; NPP-VIIRS; siting; multiple criteria evaluation; China

Citation: WEI Ye, CHEN Zuoqi, XIU Chunliang, YU Bailang, LIU Hongxing, 2019. Siting of Dark Sky Reserves in China Based on Multi- source Spatial Data and Multiple Criteria Evaluation Method. *Chinese Geographical Science*, 29(6): 949–961. https://doi.org/10.1007/s11769-019-1079-2

1 Introduction

In earlier periods of human existence, the night sky was a critical way to understand concepts of time, such as month, season or year. According to changes in the starry sky, our ancestors determined the timing of activities such as planting, harvesting and sacrifice (Williamson, 1984; Miller, 1997; Malville, 2008). In modern society, the night sky is a window, through which humans touch and understand the universe. The stars in the night sky have been used for telling stories, myths and legends, providing generations of wonderful childhood memories for people around the world (Collison and Poe, 2013). And many kinds of animals and plants live under the dark sky, such as cats, bats, epiphyllum and so on. Generally speaking, the night sky is a precious natural source for human beings and our animal friends, just as worthy of preservation as any other resource.

Received date: 2018-12-10; accepted date: 2019-04-05
Foundation item: Under the auspices of the National Natural Science Foundation of China (No. 41871162)
Corresponding author: CHEN Zuoqi. E-mail: zqchen@geo.ecnu.edu.cn

However, in recent decades many people live in cities, growing up without seeing the Milky Way and other major constellations, due to light pollution from overuse of artificial lighting tools. Astronomical observations have been disturbed, and distant ecosystems disrupted by the sky glow from cities. Some studies have demonstrated that the prevalence of light exposure may lead to physiological, epidemiological, and ecological consequences (Pauley, 2004; Navara and Nelson, 2007). The night environments of human and biosphere are being steadily eroded.

Fortunately, since the early 1970s, many concerns over the rapid growth of sky brightness and light pollution have been expressed by astronomical communities, scholars and governments (Cinzano et al., 2000). Many organizations, studies and meetings have been dedicated to this topic (Cinzano et al., 2001; Cauwels et al., 2014). The International Dark-sky Association (IDA) is the first and largest organization in the dark-sky movement, founded in 1988, and aims to preserve and protect the night environment and heritage of dark skies. As a centerpiece, the IDA promoted an International Dark Sky Places program in 2001 (IDA, 2001). The program selects and designates Dark Sky Places from many applicants around the world, and locations which become certified places derive the help and guidance from the IDA to promote work, enhance visibility and foster local astro-tourism (Collison and Poe, 2013). IDA offers five types of designations, including International Dark Sky Parks (DSP), International Dark Sky Reserves (DSR), International Dark Sky Communities (DSC), International Dark Sky Sanctuaries (DSS) and Dark Sky Developments of Distinction (DSDD). Recently, the number of applications has increased each year, demonstrating that the protection of dark sky is attracting more and more public attention. Since 2007, IDA has certified 76 places in total all around the world (IDA, 2018).

So far, there are no IDA certified Dark Sky Places in China. Ali area in Tibet, China, is still in the rigorous application process, and is widely considered as the top contender to be the first certified Dark Sky Reserve in China. As the third largest country in terms of territorial area, we believe that there must be additional suitable places to establish Dark Sky Reserves. Therefore, we attempt to identify all locations that have the potential to become a Dark Sky Place, and provide some valuable reference for creating more Dark Sky Places in China. Above all, we hope this work will attract more attention to the dark sky, especial from local governments of China. In order to make our work pertinent, we have only chosen the Dark Sky Reserve as our research object, rather than all five types of designations this time. Because, among the five types of IDA designations, the land demand is largest, the urgency of protection is strongest, and building condition is most tough for Dark Sky Reserves.

It can be difficult to find suitable places to create DSRs in such a big country. It must be determined that the place has not been polluted by artificial nightlights, possesses sufficient conservation value. Some scholars have designed instruments and fieldwork tools specifically for measuring light pollution (Cinzano, 2004; Nurbandi et al., 2016). The determination of sky quality by the IDA depends primarily on the results of fieldwork (IDA, 2018). Compared with the fieldwork measurements, nighttime light remote sensing is suitable to obtain large-scale and high numbers of artificial lighting data with low costs (Li et al., 2013; Li and Li, 2014; Chen et al., 2017; Jechow et al., 2017; Jiang et al., 2017; Hänel et al., 2018). According to previous studies, there are two kinds of commonly used sensors for monitoring light pollution on earth: DMSP-OLS and NPP-VIIRS. The Operational Linescan System (OLS), which boards on Defense Meteorological Satellite Program (DMSP) satellites, has a broad spectral response from visible band signals (440–940 nm), enabling direct measurement of upward light emissions from Earth's surface. The Visible Infrared Imaging Radiometer Suite (VIIRS), carried by the Suomi National Polar-orbiting Partnership (NPP) satellite, is another important sensor, which can provide light pollution information other than DMSP-OLS. Compared with the DMSP-OLS, data acquired from the NPP-VIIRS has higher spatial resolution (about 500 m) and sensitivity to very low levels of visible light (to ~2×10^{-9} w / ($cm^2 \times$ sr) (Miller et al., 2006, 2013; Hillger et al., 2013; Shi et al., 2014). These improvements make NPP-VIIRS more suitable for detecting areas disturbed by artificial lights. Therefore, some scholars have recently started to use NPP-VIIRS data to monitor light pollution, such as Duriscoe et al. (2018) and Nurbandi et al. (2016).

Some scholar attempted to use high-resolution nighttime light imagery to investigate the artificial light pollution, like JL1-3B, EROS-B, Luojia 1-01(Kyba et al., 2015; Jiang et al., 2018; Zheng et al., 2018). Compared with DMSP-OLS and NPP-VIIRS, the high-resolution data could reveal more spatial details of artificial light. However, the scopes of high-resolution images are often very small, which is not suitable for large-scale monitoring. Besides, these data are not always freely available for acquisition. Thus, NPP-VIIRS is a relatively appropriate data source at present for investigating the light pollution in such a large research area as China.

However, less pollution by artificial light is merely a constraint condition for a true DSR, and there are many other important factors to consider to become a true DSR, e.g., whether the transportation is convenient or whether the land can have other compatible use value (Rodrigues et al., 2015; Hearnshaw, 2015). Unfortunately, most researches based on remote sensing method had focused on light pollution or the quality of the night sky, while other factors were rarely concerned about. Accordingly, under the framework of IDA requirements, and with reference to construction experiences of existing DSRs, the authors attempt to use multi-source spatial data to select suitable places for constructing dark sky reserves in China, from a macroscopic and comprehensive perspective.

2 Materials and Methods

2.1 Data and study area

2.1.1 NPP-VIIRS data

In this paper, NPP-VIIRS nighttime light data were obtained from the Earth Observation Group (EOG), National Geophysical Data Center (NGDA) at National Oceanic and Atmospheric Administration (NOAA) to identify areas less polluted by artificial lights. So far, two kinds of temporal averaging NPP-VIIIRS data can be obtained from EOG, namely monthly and annual composites. The monthly composites have not been filtered to screen out lights from auroras, fires, boats, and other temporal sources. In contrast, the annual composites have removed temporal lights and background (non-light) values. In addition, a month is too short to understand climate conditions for a certain area. The annual composites are more useful for our studies; therefore we chose annual composites as the basic data.

Currently, only annual composite data from 2015 can be downloaded from the EOG website, in a folder consisting of four kinds of files. Files with field 'vcm-orm' (VIIRS Cloud Mask-Outlier Removed) contain cloud-free average radiance values, which have undergone an outlier removal process to filter out fires and other ephemeral lights; Files with field 'vcm-orm-ntl' (VIIRS Cloud Mask-Outlier Removed-Nighttime Lights) contain the 'vcm-orm' average, with background (non-lights) set to zero; 'vcm-ntl' (VIIRS Cloud Mask-Nighttime Lights) files contain the 'vcm' average, with background (non-lights) set to zero. Files with the extension 'cvg' are integer counts of total coverages or observations available, regardless of cloud-cover. This paper applied 'vcm-orm-ntl' (hereinafter referred to as 'VON data') and 'cvg' ('CVG data') data, with the former used to show the strength of artificial light influence, and the latter to assess the climate condition suitability for observing the night sky.

2.1.2 Transportation data

According to Dark Sky Reserve Program Guidelines (IDA, 2018), an IDA qualified Dark Sky Reserve (DSR) should possess a distinguished quality of starry nights and a good nocturnal natural environment, regarded as precious resources enjoyed by the public. Eco-tourism and astro-tourism are encouraged by the DSR, which is beneficial to the comprehensive utilization of land (Liu et al., 2018). Therefore establishing dark sky reserves in areas where it is hard for human beings to set foot is meaningless. The DSR aims at building interesting and attractive areas, rather than depopulated zones. Thus, we took traffic accessibility into consideration. Railway and major road lines in China were obtained from Baidu Map, to assess traffic accessibility.

2.1.3 Landscape and famous scenery data

In addition to the quality of night sky, possession of sufficient natural or human resources and a beautiful ecological environment can obviously increase the attractiveness and competitiveness of a DSR. In order to measure the natural endowment of candidate areas, this paper introduced landscape and famous scenery data as the basis of analysis. In China, landscape and famous sceneries are places with beautiful environments and ornamental, cultural or scientific value according to the Regulations on Scenic Spots and Historic Sites of China. As of August 2017, China approved a total of 225 national landscape and famous sceneries, which are theoretically the top scenic spots in China. DSRs located close to or in such scenic spots will inevitably enjoy the positive external effects they bring, enhancing DSR attraction.

The list of national landscapes and famous sceneries used in this article was derived from the official website of the Housing and Urban-rural Development department of the People's Republic of China, with location information obtained through Baidu coordinate tools.

2.1.4 *Data preparation*

For compatibility, all data were projected into the Lambert Azimuthal Equal Area Projection. VON and CVG data were resampled to 500 m spatial resolution and extracted by the mask of China.

2.1.5 *Study area*

The study area is China, which has the world's largest population and is undergoing the fastest urbanization on the planet. Along with the rapid increase of population and urbanization, many excellent night environments are being eroded (Yang et al., 2019). Therefore, it is urgent to provide appropriate protection to areas unaffected by light pollution.

2.2 Methods

2.2.1 *Fishnet*

According to IDA guidelines (IDA, 2018), the minimum land size of a DSR should be larger than 700 km^2 around a 15-km radius core area. In raster data, the 15-km radius circular region is exactly corresponding to 30 km × 30 km pixel (minimum enclosing rectangle). Referencing these factors, we divided the research area into over ten thousand 30 km × 30 km rectangular grids (or cells), by using the Create Fishnet function of ArcGIS 10.2. Then, appropriate grids were chosen as locations of DSRs, referred to as 'optional grids' herein.

2.2.2 *Zonal geometry*

Zonal geometry is a built-in function of ArcGIS 10.2, calculating specific geometric measures for each zone in a dataset, including area, perimeter, thickness, and ellipse characteristics (Ebdon, 2001). Thickness (in pixels) measures the deepest (or thickest) point within a zone. In other words, thickness is the radius of the maximum circle that could be drawn within a certain area without any external pixels. The schematic diagram of thickness is shown in Fig.1.

To retain sufficient space to build core and buffer areas, it is necessary to find a sizeable, neat-shaped and continuous location for DSRs. The thickness index can meet this demand, as larger thickness indicates sufficient buffer space to protect the core area from night light pollutions.

2.2.3 *Traffic accessibility*

Based on the major railway and road lines, the traffic accessibility was measured by the distance to road or railway for each grid option.

2.2.4 *Attractiveness*

Attractiveness was measured by the distance to the nearest landscape and famous scenery for each optional grid in ArcGIS 10.2.

2.2.5 *Multiple criteria evaluation*

The siting of DSRs involves many factors/conditions, and therefore can be conceptualized as a multiple criteria evaluation problem (Sui, 1993). To obtain comprehensive evaluation results, each factor/condition should be taken into consideration and weighed according to relative importance. The weight of each factor can be estimated utilizing a pairwise comparison matrix (PWCM), constructed according to the pairwise comparison method, also known as the analytical hierarchy process (AHP), a commonly used method in multiple criteria evaluation (Saaty, 1980; Khoi and Murayama, 2010).

2.3 Technique process

2.3.1 *Constraint condition*

A basic requirement for all DSRs, according to the IDA, is that an area must be polluted by minimal artificial

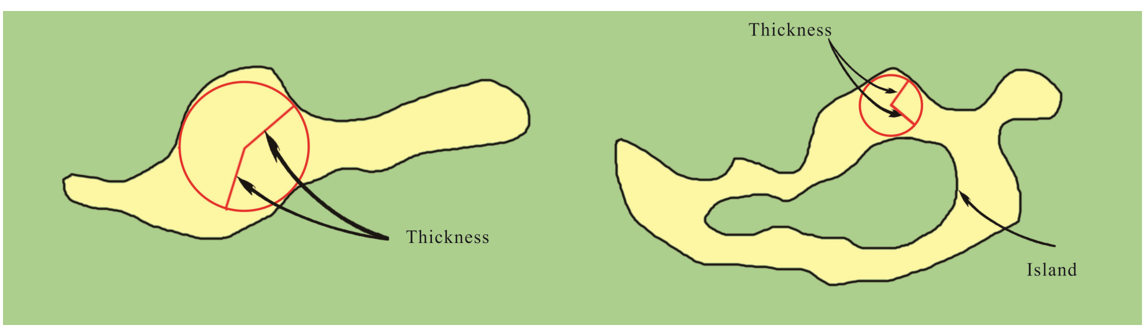

Fig. 1 Schematic diagram of thickness

light. The IDA has classified nighttime environments into three levels/tiers: gold, silver and bronze (IDA, 2018). Gold level corresponds to natural, non-polluted or near-natural night skies; silver corresponds to minor impact from light pollution; bronze corresponds areas that cannot meet the silver level, but still offer a relatively comfortable nocturnal environment. IDSR guidelines (IDA, 2018) require that the core night sky quality of DSRs fit one of the three tiers (gold, silver or bronze). Although the evaluation of sky quality needs long-term fieldwork, NPP-VIIRS data can be employed to conduct primary screening jobs.

Another scale for sky darkness, Bortle's Dark Sky Scale, was created by John Bortle and published in the February 2001 issue of Sky and Telescope. The scale categorizes nine Bortle Sky Classes, which correspond with IDA tiers. For example, the silver tier corresponds to Bortle Sky Classes 3–5, and the bronze tier corresponds to classes 5–6 (IDA, 2018). Nurbandi et al. (2016) found that radiance values in range of 0.207987×10^{-9}~0.69997×10^{-9} W/(cm^2×sr) corresponded to Bortle Sky Class 4, and 23.814596 to 44.069031 W/(cm^2×sr) corresponded to Class 8. Therefore, for the sky darkness to achieve silver level, the radiance value must be less than 1×10^{-9} W/(cm^2×sr). However, the Minimum Detectable Signal of NPP-VIIRS is ~2×10^{-9} W/(cm^2×sr) (Miller et al., 2013). That is, the threshold must be set as 0 for the annual composited NPP-VIIRS data to meet the requirement of silver level.

Besides light pollution, climate condition is also an important factor to consider, which indicates the number of cloudless days in a year. NPP-VIIRS also offers CVG data (See 2.1.1) to explore this question. Thus, there are two constraint conditions in total: light condition and climate condition. To explore the conditions and identify optional grids for building DSRs, a technical process appropriate to the ArcGIS 10.1 platform was designed (Fig. 2).

As shown in Fig.2, we used the sum of the DN values of VON data in each grid (30 km × 30 km) to determine the light condition, and employed the average DN of CVG data to determine the climate condition. Only the grids that met the conditions Sum(DN) = 0 in VON data and Avg(DN) >100 in CVG data were identified as optional grids.

2.3.2 Suitable conditions

To become a DSR, simply no nighttime light pollution and a good climate condition are not sufficient. More conditions are further needed to judge whether a place is suitable to build a DSR.

Up until now, the IDA has certified 11 DSRs worldwide according to the official Dark Sky Reserves website: http://www.darksky.org/idsp/reserves/. Certification standards are very strict and involve a lengthy review process. As an applicant, it is first necessary to meet the five qualification aspects, including excellent dark sky quality, sufficient land area and appropriate shape, a 'peripheral' or 'buffer' area, open access for public and comprehensive value. The above five qualification aspects are clearly reflected in the DSR profiles. In terms of area, the smallest DSR is Kerry in Ireland, with an area is 700 km^2, and the largest DSR is Aoraki Mackenzie, New Zealand, whose area is 4367 km^2. Both locations were able to meet the technical requirements of building core and buffer areas, and although IDA does not have a clear minimum area requirement, it is clear that the larger the area, the more favorable the protection of the dark sky and related activities.

In terms of the night sky quality, all DSRs are above the silver level. In terms of public access, most DSRs describe traffic convenience in their profile. For instance, Brecon Beacons National Park 'is within easy access of over a million people', and Moore's Reserve 'offers authentically dark nighttime outdoor experiences to over ten million people who live within a two-hour train journey of the Downs'.

In comprehensive value, most DSRs have more than one function. For example, Exmoor and Snowdonia are of the 15 national parks in the UK, where protected

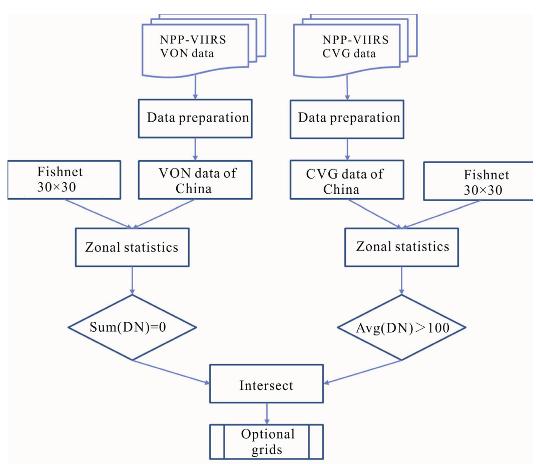

Fig. 2 The technique process of selecting optional grids by using constraint conditions

landscapes are recognized for their diversity and scenic quality. Also, Pic du Midi is nationally and internationally recognized as a famous attraction. This implies that, with reference to the IDA requirement for eligibility and relevant experience, in addition to night sky quality, other suitable conditions should be proposed to find ideal areas to build DSRs. These conditions mainly include scale, traffic, ecological and attractiveness conditions (Table 1). For each condition, we design specific indexes to perform quantificational estimations.

2.3.3 Establishment of finalist database

Based on the constraint and suitable conditions, we identified certain places that are most suitable for constructing DSRs. We then built a finalists' database that stores related information for these places, to provide valuable reference for locating DSRs or other types of dark sky places in the future.

3 Result Analysis

3.1 Analysis of constraint conditions

Following the technical route proposed in 2.3.1, the constraint condition for constructing DSRs was analyzed. The result is shown in Fig. 3, in which Fig. 3(a) delineates the spatial distribution of the 30 km × 30 km grids which suffered less light pollution, Fig. 3(b) shows the spatial distribution of grids with more cloud-free days, and Fig. 3(c) shows the results of intersecting lighting and cloud conditions, or the fishnets where weather and light pollution are ideal. Thus, we defined these fishnets as optional grids. We extracted a total of 2647 such optional grids.

Table 1 Indexes for suitable conditions

Condition	Index	Description
Scale	Thickness	The consecutive-range characteristic of the optional grid
Traffic	Traffic accessibility (distance to the nearest main railway or road)	Ease of approachability for people or tourists into the region
Attractiveness	Distance to the nearest landscape and famous scenery	In addition to observing the starry sky, the other elements of attracting visitors

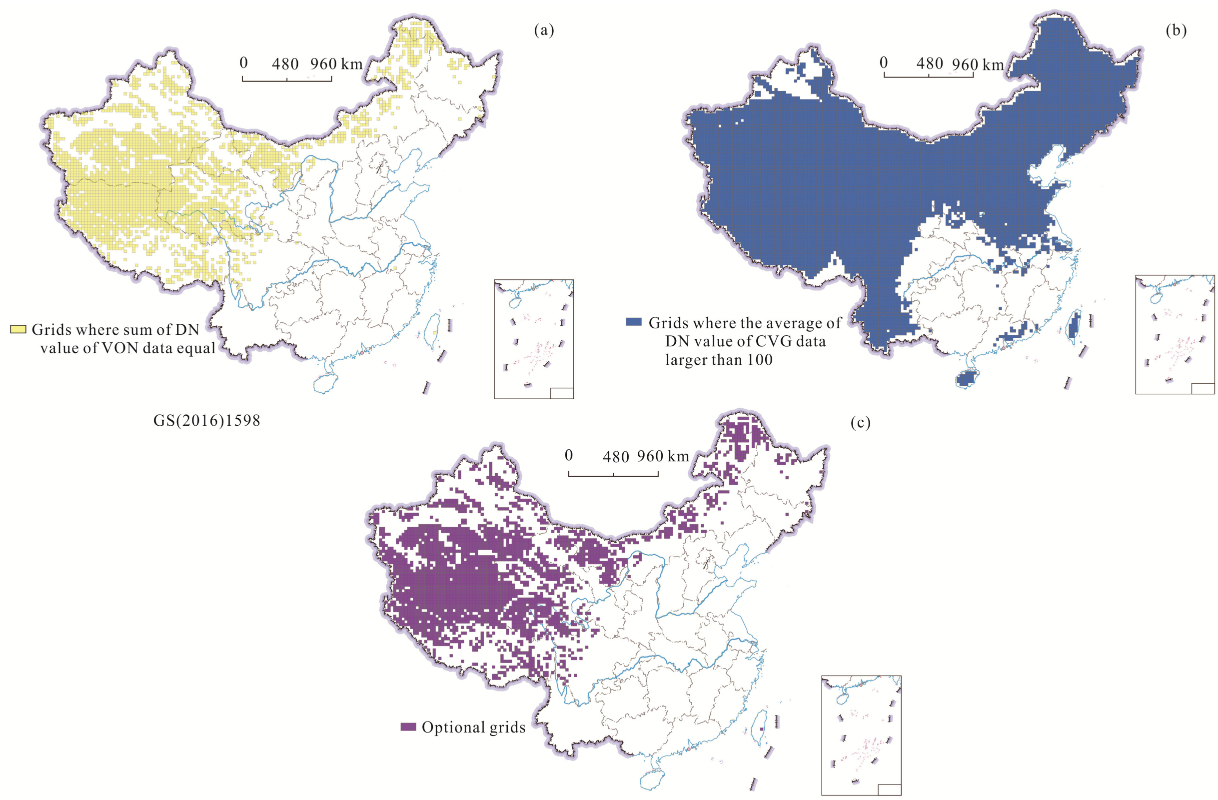

Fig. 3 Fishnets meeting constraint conditions

As shown in Fig.3, due to the influence of mainland monsoon-type climates, the areas with more cloud free days were primarily located in the western and northern areas of China. The grids where the sum DN values of VON data equaled 0 were also mainly in the west and north areas of China, with more sparse distribution of cities and populations and less serious light pollution. From Fig. 3(b), it can be seen that meteorological observation conditions in Taiwan, Hainan and Guangdong were not worse than those in the northern region, but few appropriate optional grids were identified, because light pollution is not optimistic in these economically developed areas.

3.2 Analysis of suitable conditions

3.2.1 Scale condition

In theory, the larger the protected area, the more favorable it is ability to protect the dark night. However, it is not enough to measure scale condition by relying only on area size alone. The reason is, even if there is a large but narrow continuous area, the core area is easily disturbed by outside interference sources through the narrow sections. Therefore, the thickness scale was utilized in addition to the fishnet minimum area constraint. As mentioned above, the most important function of thickness is the ability to determine whether there is a deep area in a continuous patch.

First, all adjacent optional grids were dissolved into continuous joint areas, and then the thicknesses of these joint areas were measured. Thickness helps identify which areas have more spatial buffer capacity against external light pollution, and therefore are more suitable for building and management of DSRs.

Fig. 4 shows the thickness calculation results of each joint area. According to the principle of thickness calculation, if one grid is isolated from other grids, it has a thickness of in the minimum thickness of all joint areas. The maximum values of thickness are mainly distributed in the west of Tibet, the southern part of Xinjiang and the western and northern parts of Qinghai. The second largest values are mainly distributed in the eastern part of Qinghai, and the easternmost and westernmost of Inner Mongolia. The distribution of other values is relatively extensive and fragmented.

3.2.2 Traffic condition

A DSR is protected not only for science, but also for education and public involvement. Therefore, traffic accessibility is an important factor to consider in DSR siting. Based on the method introduced in 2.2.3, the traffic accessibility of each optional grid was measured, with results shown in Fig.5. Obviously, the accessibility to core areas of Qinghai-Tibet Plateau and Tarim Basin is very low. In this sense, there is little meaning to build DSRs in such areas, which are difficult for common people to access now and in the near future. Thus, we strongly recommend building DSRs in areas with high traffic accessibility.

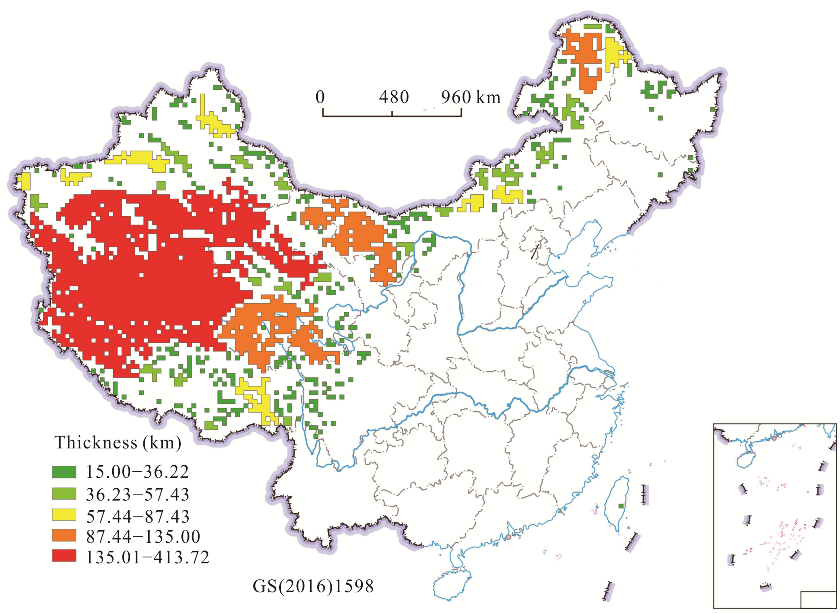

Fig. 4 Scale condition: thicknesses of joint areas

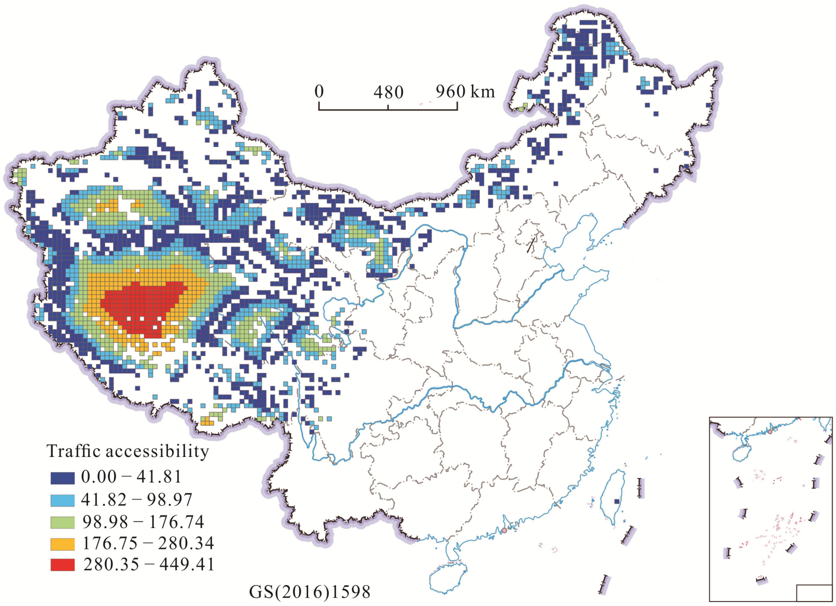

Fig. 5 Traffic condition: distance to the nearest main railway or road

3.2.3 Attractiveness condition

Fig. 6 shows the distance between each optional grid and the nearest landscape and famous scenery, reflecting whether the optional grid has additional resources to attract viewers to the area, other than the high-quality night sky. The smaller the distance, the greater the grids enjoy positive externalities from landscape and famous sceneries, improving the visibility and attractiveness of the DSR.

3.3 Suitability assessment

A suitability assessment was made for each optional grid, according to the suitable condition. First of all, the three suitability indicators, traffic, attractiveness and scale, were normalized, generating a value that belongs to [0, 1]. For the scale condition, we used formula (1); for traffic and attractiveness conditions, we used formula (2):

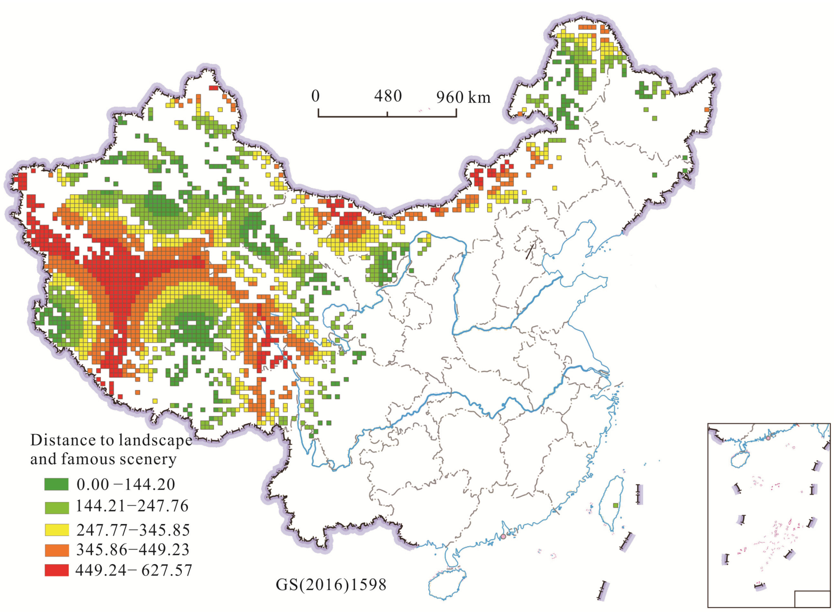

Fig. 6 Attractiveness condition: distance to the nearest landscape and famous scenery

$$y = \frac{x - x_{min}}{x_{max} - x_{min}} \quad (1)$$

$$y = \frac{x_{max} - x}{x_{max} - x_{min}} \quad (2)$$

where y stands for the normalized value, x stands for the original value, x_{max} stands for the maximum x value, and x_{min} stands for the minimum x value.

Then, the PWCM method was used to determine the weight of each suitable condition indicator (see 2.2.5). In the pairwise comparison matrix, the relative importance of two conditions was rated regarding the suitability of DSR, using a scale with values from 9 to 1/9. A rating of 9 indicates that in relation to the column factor, the row factor is more important, and a rating of 1/9 indicates that, relative to the column factor, the row factor is less important. In cases where the column and row conditions are equally important, both have a rating value of 1. A team of 10 experts determined the ratings of the conditions, applying a majority rule to reach agreement in comparing the relative importance. The weights of the conditions were then calculated from the PWCM, which is shown in Table 2. The consistency ratios (CRs) of 0.00 were within the acceptable level (Saaty, 1990).

According to the pairwise comparison matrix, the weighted sum of scale condition, traffic condition and attractiveness condition (0.2856 × traffic + 0.2856 × attractiveness + 0.4288 × scale) was taken as comprehensive evaluation score of the suitability of the optional grid. The visualization results are shown in Fig.7.

3.4 Most suitable sites for DSR

The grids with comprehensive evaluation scores larger than 0.6 were extracted from optional grids as the most suitable sites for DSRs (Fig.7). As shown in Fig.8, the most suitable sites, namely 1443 grids (30 km × 30 km), were mainly distributed in Tibet (510), Xinjiang (674), Qinghai (197), Gansu (41) and Inner Mongolia (21). In detail, the distribution was more concentrated in Tibet, Xinjiang and Qinghai, while more fragmented in Gansu and Inner Mongolia. In addition, as shown in Fig.8, the Ali area of Tibet mentioned above is located in our most suitable sites, showing that our findings are scientific and have practical reference value.

3.5 The landscape diversity of the most suitable sites for DSR

Different ground landscape backgrounds could produce different visual experiences of the starry sky. Thus, IDA consciously considered the diversity of the ground landscape when selecting the DSRs. For instance, The Mackenzie basin reserve in New Zealand is dominated by grasslands. And Kerry DSR in Ireland is featured by

Table 2 Pairwise comparison matrix for evaluating the relative importance of each condition

	Traffic	Attractiveness	Scale	Weight
Traffic	1	1	2/3	0.2856
Attractiveness	1	1	2/3	0.2856
Scale	3/2	3/2	1	0.4288
Consistency ratio (CR) = 0.00				

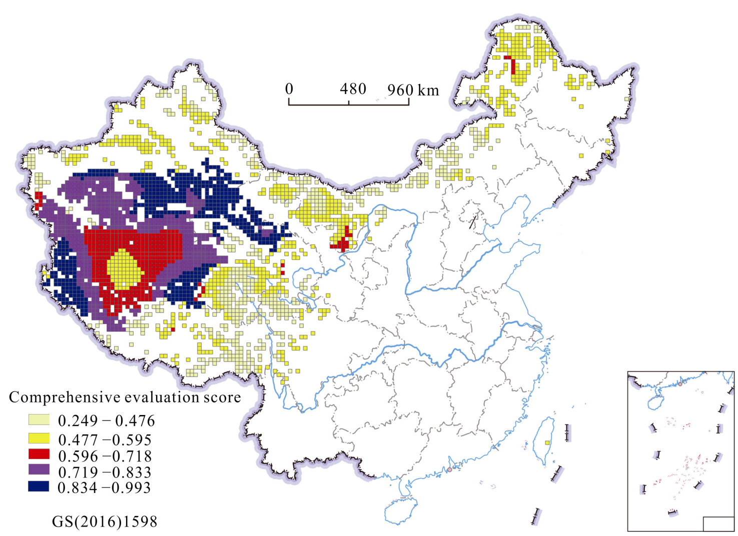

Fig. 7 Comprehensive evaluation score for each optional grid based on the three suitable conditions

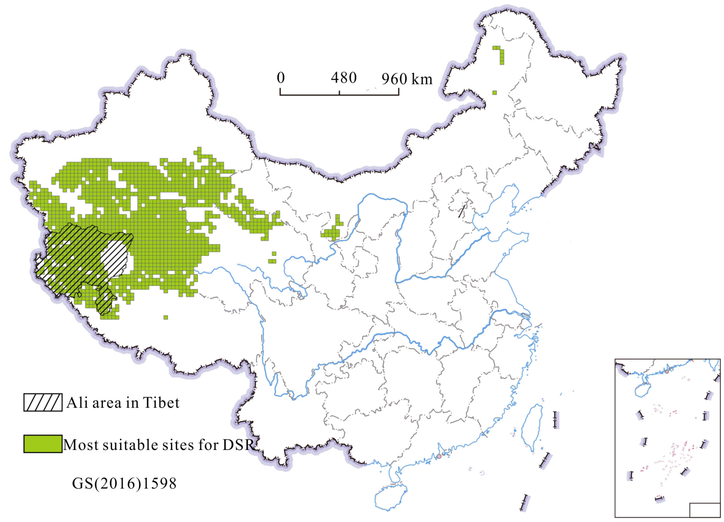

Fig. 8 Most suitable sites for building Dark Sky Reserves

Kerry mountain and Atlantic Ocean. To investigate how many ground landscape types could be selected for establishing DSR in China, global land cover data from the Food and Agriculture Organization (FAO) Global Land Cover SHARE (GLC-SHARE) database (Latham et al., 2014) and 1∶4 000 000 land geomorphology map of China (Zhou and Cheng, 2014) were employed to perform an overlay analysis with 30 km × 30 km fishnets in the ArcGIS platform. Through the overlay analysis, the main land cover type and main land geomorphology type for each most suitable fishnet were determined by majority principle. The relevant summary results are shown in Table 3 and Table 4.

As shown in Table 3, there are totally seven land cover types for the most suitable fishnets (For the whole of China, the figure is 11). Most of fishnets are dominated by Grassland, a certain number of fishnets are covered by Sparse vegetation and Bare soil, and only a small proportion of fishnets are featured by other landscape types. According to the morphology and genesis (Zhou and Cheng, 2014), the land geomorphologies of the most suitable fishnets could be divided into 57 types which are listed in Table 4. On the whole, the landscape types for the most suitable sites are very abundant. That is to say, China has the potential to establish multiple types of Dark Sky Reserves. But it is worth noting that about 30% of the fishnets are located at low or medium altitude (< 2000 m), while most of the fishnets are located at high or extreme high altitude (>2000 m). This may also be an important challenge for building DSRs in China.

4 Discussion

Obviously, the siting and designation of DSRs is complex, tough work. This article only discusses the siting conditions of DSRs from the aspects of light pollution degree, meteorological observation condition, land construction, traffic accessibility and scenic attraction. In fact, there are other requirements to become a certified DSR according to IDA Dark Sky Reserve program guidelines, including night sky protection measures, night management measures, public education, etc (Rodrigues et al., 2015). Therefore, this siting analysis merely aims to provide a location reference for DSR construction, and selected areas cannot be definitely used, rather serve as "options" that may have high potential. Conversely, unselected areas may also become suitable to build DSRs in the future, through land consolidation, lighting management and other means (Hearnshaw, 2015). Even so, this study greatly narrows the scope of the search, saving a lot of early inspection work, and provides a valuable reference for actual DSR location work.

Table 3 Land cover type of most suitable sites for building Dark Sky Reserves

Land cover type	Number of fishnets
Bare soil	214
Grassland	889
Shrubs Covered Areas	1
Snow and glaciers	10
Sparse vegetation	320
Tree covered areas	7
Water bodies	2

Table 4 Land form type of most suitable sites for building Dark Sky Reserves

Land geomorphology type	Number of fishnets	Land geomorphology type	Number of fishnets	Land geomorphology type	Number of fishnets
Extremely high altitude great relief mountains	21	High altitude outwash drip plain	37	Middle altitude dry-diluvial plain	46
Extremely high altitude middle relief mountains	1	High altitude plain of denudation	14	Middle altitude hills	26
Extremely high altitude relief mountains	86	High altitude relief mountains	87	Middle altitude lacustrine plain	1
High altitude alluvial plain	1	High altitude small relief mountains	169	Middle altitude loess liang-mao	3
High altitude alluvial-diluvial plain	33	Lake	11	Middle altitude Middle relief mountains	7
High altitude alluvial-diluvial platform	3	Low altitude aeolian landform	24	Middle-high altitude alluvial-diluvial plain	10
High altitude alluvial-diluvial-lacustrine platform	12	Low altitude alluvial plain	21	Middle-high altitude alluvial-diluvial platform	4
High altitude denudation platform	3	Low altitude alluvial-diluvial plain	4	Middle-high altitude denudation platform	2
High altitude diluvial plain	88	Low altitude denudation plain	4	Middle-high altitude diluvial plain	12
High altitude diluvial platform	1	Low altitude diluvial plain	4	Middle-high altitude diluvial-lacustrine plain	3
High altitude diluvial-lacustrine plain	44	Low altitude diluvial-lacustrine plain	7	Middle-high altitude dry-diluvial plain	19
High altitude drift plain	6	Low altitude dry-diluvial plain	4	Middle-high altitude hills	1
High altitude great relief mountains	15	Low altitude hills	2	Middle-high altitude loess liang-mao	3
High altitude hills	73	Low altitude lacustrine plain	19	Middle-high altitude Middle relief mountains	17
High altitude lacustrine plain	23	Middle altitude aeolian landform	236	Middle-high altitude plain of denudation	3
High altitude lacustrine platform	3	Middle altitude alluvial plain	4	Middle-high altitude relief mountains	17
High altitude lava accumulational plain	1	Middle altitude alluvial-diluvial plain	15	Middle-high altitude saline plain	4
High altitude lava accumulational platform	3	Middle altitude denudation plain	10	Modern glacier	11
High altitude middle relief mountains	152	Middle altitude diluvial-lacustrine plain	1	Sand dune	12

Considering the questions and difficulties aroused in this study, the research team will carry out the following work in the future:

(1) Comprehensively collect information on economic development, population distribution, natural environment and social management of potential DSR areas, to establish a more detailed DSR spatial selection database.

(2) For areas of particularly strong suitability, carry out detailed fieldwork on light pollution and make more accurate assessments.

Above all, the construction of DSRs requires not only the prevention and control of light pollution, but also the enhancement of people's awareness of the protection of night sky resources and the attention of government. In addition, the development of Dark Sky Parks, Dark Sky Communities, Dark Sky Sanctuaries and other Dark Sky protecting entities should also be encouraged in China, so that more people to get involved in appreciating and protecting the night sky.

5 Conclusions

Based on the annual composited NPP-VIIRS data and other spatial data, a siting analysis was conducted on Dark Sky Reserves in China. A condition-based analytical framework was built by employing fishnet, traffic accessibility, zonal geometry and other basic GIS spatial analysis methods. According to our findings, about 75% of the land in China is polluted by artificial light to some degree. Considering light pollution and weather conditions, combined with minimum size of DSR construction (30 km × 30 km), only 24.82% of the land in China could be used, and less than 13% was suitable to build a DSR. With the rapid expansion of urban area, this figure decreases year by year. The spatial distribution found that ideal lands for DSRs are mainly distributed in western and northern China, including Tibet, Xinjiang, Qinghai, Gansu and Inner Mongolia. There are large differences in surface landscape types in these areas, which is helpful for building DSRs with different characteristics.

References

Cauwels P, Pestalozzi N, Sornette D, 2014. Dynamics and spatial distribution of global nighttime lights. *EPJ Data Science*, 3(1): 2. doi: 10.1140/epjds19

Chen Z Q, Yu B L, Song W et al., 2017. A new approach for detecting urban centers and their spatial structure with nighttime light remote sensing. *IEEE Transactions on Geoscience and Remote Sensing*, 55(11): 6305–6319. doi: 10.1109/TGRS. 2017.2725917

Cinzano P, Falchi F, Elvidge C D et al., 2000. The artificial night sky brightness mapped from DMSP satellite operational linescan system measurements. *Monthly Notices of the Royal Astronomical Society*, 318(3): 641–657. doi: 10.1046/j.1365-8711.2000.03562.x

Cinzano P, Falchi F, Elvidge C D, 2001. The first world atlas of the artificial night sky brightness. *Monthly Notices of the Royal Astronomical Society*, 328(3): 689–707. doi: 10.1046/ j.1365-8711.2001.04882.x

Cinzano P, 2004. A portable spectrophotometer for light pollution measurements. *Memorie Della Società Astronomica Italiana Supplement*, 5: 395–398.

Collison F M, Poe K, 2013. 'Astronomical tourism': the astronomy and dark sky program at Bryce canyon national park. *Tourism Management Perspectives*, 7: 1–15. doi: 10.1016/ j.tmp.2013.01.002

Duriscoe D M, Anderson S J, Luginbuhl C B et al., 2018. A simplified model of all-sky artificial sky glow derived from VIIRS Day/Night band data. *Journal of Quantitative Spectroscopy and Radiative Transfer*, 214: 133–145. doi: 10.1016/j.jqsrt. 2018.04.028

Ebdon D, 1985. *Statistics in Geography*. 2nd ed. Oxford: Blackwell.

Hänel A, Posch T, Ribas S J et al., 2018. Measuring night sky brightness: methods and challenges. *Journal of Quantitative Spectroscopy and Radiative Transfer*, 205: 278–290. doi: 10.1016/j.jqsrt.2017.09.008

Hearnshaw J, 2015. The Aoraki Mackenzie international dark sky reserve and light pollution issues in New Zealand. In: *IAU General Assembly*. IAU, 22, Hawaii.

Hillger D, Kopp T, Lee T et al., 2013. First-light imagery from Suomi NPP VIIRS. *Bulletin of the American Meteorological Society*, 94(7): 1019–1029. doi: 10.1175/BAMS-D-12-00097.1

International Dark-Sky Association (IDA), 2001. The International Dark Sky Places conservation program recognizes and promotes excellent stewardship of the night sky. http://www.darksky.org/idsp/. Cited 10 March 2018.

International Dark-Sky Association (IDA), 2018. Dark sky reserve program guidelines. https://www.darksky.org/wp-content/uploads/2018/12/IDSR-Guidelines-2018.pdf. Cited 3 May 2019.

Jechow A, Kolláth Z, Ribas S J et al., 2017. Imaging and mapping the impact of clouds on skyglow with all-sky photometry. *Scientific Reports*, 7(1): 6741. doi: 10.1038/s41598-017-06998-z

Jiang W, He G J, Long T F et al., 2017. Assessing light pollution in China based on nighttime light imagery. *Remote Sensing*, 9(2): 135. doi: 10.3390/rs9020135

Jiang W, He G J, Long T F et al., 2018. Potentiality of using Luojia 1-01 nighttime light imagery to investigate artificial light pollution. *Sensors*, 18(9): 2900. doi: 10.3390/s18092900.

Khoi D D, Murayama Y, 2010. Delineation of suitable cropland areas using a GIS based multi-criteria evaluation approach in the Tam Dao national park region, Vietnam. *Sustainability*, 2(7): 2024–2043. doi: 10.3390/su2072024

Kyba C C M, Garz S, Kuechly H et al., 2015. High-resolution imagery of earth at night: new sources, opportunities and challenges. *Remote Sensing*, 7(1): 1–23. doi: 10.3390/rs 70100001

Latham J, Cumani R, Rosati I et al., 2014. FAO global land cover (GLC-SHARE) beta-release 1.0 database, land and water division. http://www.fao.org/uploads/media/glc-share-doc.pdf. Citied 3 December 2018.

Li X, Chen F R, Chen X L, 2013. Satellite-observed nighttime light variation as evidence for global armed conflicts. *IEEE Journal of Selected Topics in Applied Earth Observations and Remote Sensing*, 6(5): 2302–2315. doi: 10.1109/JSTARS. 2013.2241021

Li X, Li D R, 2014. Can night-time light images play a role in evaluating the Syrian Crisis? *International Journal of Remote Sensing*, 35(18): 6648–6661. doi: 10.1080/01431161.2014. 971469

Liu J, Wang J, Wang S H et al., 2018. Analysis and simulation of the spatiotemporal evolution pattern of tourism lands at the Natural World Heritage Site Jiuzhaigou, China. *Habitat International*, 79: 74–88. doi: 10.1016/j.habitatint.2018.07.005

Malville J M, 2008. *Guide to Prehistoric Astronomy in the Southwest*, *Revised and Updated*. Boulder, CO: Johnson Printing Company.

Miller D S, 1997. *Stars of the First People*: *Native American Star Myths and Constellations*. Bel Air, CA: Westwinds Press.

Miller S D, Hawkins J D, Kent J et al., 2006. NexSat: previewing NPOESS/VIIRS imagery capabilities. *Bulletin of the American Meteorological Society*, 87(4): 433–446. doi: 10.1175/BAMS-87-4-433.

Miller S D, Straka III W, Mills S P et al., 2013. Illuminating the capabilities of the Suomi national polar-orbiting partnership (NPP) visible infrared imaging radiometer suite (VIIRS) day/night band. *Remote Sensing*, 5(12): 6717–6766. doi: 10.3390/rs5126717

Navara K J, Nelson R J, 2007. The dark side of light at night: physiological, epidemiological, and ecological consequences. *Journal of Pineal Research*, 43(3): 215–224. doi: 10.1111/j.1600-079X.2007.00473.x

Nurbandi W, Yusuf F R, Prasetya R et al., 2016. Using visible infrared imaging radiometer suite (VIIRS) imagery to identify and analyze light pollution. *IOP Conference Series*: *Earth and Environmental Science*, 47: 012040. doi: 10.1088/1755-1315/47/1/012040

Pauley S M, 2004. Lighting for the human circadian clock: recent research indicates that lighting has become a public health issue. *Medical Hypotheses*, 63(4): 588–596. doi: 10.1016/j.mehy.2004.03.020

Rodrigues A L O, Rodrigues A, Peroff D M, 2015. The sky and sustainable tourism development: a case study of a dark sky reserve implementation in Alqueva. *International Journal of Tourism Research*, 17(3): 292–302. doi: 10.1002/jtr.1987

Saaty T L, 1980. *The Analytic Hierarchy Process*: *Planning*, *Priority Setting*, *Resource Allocation*. New York: McGraw-Hill.

Shi K F, Yu B L, Huang Y X et al., 2014. Evaluating the ability of NPP-VIIRS nighttime light data to estimate the gross domestic product and the electric power consumption of China at multiple scales: a comparison with DMSP-OLS data. *Remote Sensing*, 6(2): 1705–1724. doi: 10.3390/rs6021705

Sui D Z, 1993. Integrating neural networks with GIS for spatial decision making. *Operational Geographer*, 11(2): 13–20.

Williamson R A, 1984. *Living the Sky*: *The Cosmos of the American Indian*. Norman, OK: University of OklahomaPress.

Yang J, Guo A D, Li Y H et al., 2019. Simulation of landscape spatial layout evolution in rural-urban fringe areas: a case study of Ganjingzi district. *GIScience & Remote Sensing*, 56(3): 388–405, doi: 10.1080/15481603.2018.1533680.

Zheng Q M, Weng Q H, Huang L Y et al., 2018. A new source of multi-spectral high spatial resolution night-time light imagery—JL1-3B. *Remote Sensing of Environment*, 215: 300–312. doi: 10.1016/j.rse.2018.06.016

Zhou Chenghu, Cheng Weiming, 2014. *China 1*:*4 Million Digital Landform Data Set*. (in Chinese)